PNAS
www.pnas.org

Supplementary Information for

ATP7A delivers copper to the lysyl oxidase family of enzymes and promotes tumorigenesis and metastasis

Vinit Shanbhag, Kimberly Jasmer-McDonald, Sha Zhu, Adam L. Martin, Nikita Gudekar, Aslam Khan, Erik Ladomersky, Kamlendra Singh, Gary A. Weisman, Michael J. Petris.

Michael J. Petris
Email: petrism@missouri.edu

This PDF file includes:

Supplementary Materials and Methods
Figs. S1 to S7
Captions for movies S1 and S2
Supplementary References

Other supplementary materials for this manuscript include the following:

Movies S1 and S2

SUPPLEMENTARY MATERIALS AND METHODS

Soft agar colony forming assay

The soft agar colony formation assay was performed as described previously (1).

Second Harmonic Generation Imaging Microscopy (SHGIM)

Second harmonic generation (SHG) images were acquired using a Leica SP8 confocal microscope equipped with a tunable Ti:Sapphire femtosecond laser (MaiTai DeepSee, Spectra Physics, Irvine, CA). To induce SHG, the laser wavelength was set to 880 nm. To achieve maximum excitation efficiency at the level of the sample, the laser beam was directed through a group velocity dispersion compensator. A 40x (NA=1.3) oil immersion objective was used for focusing the laser beam. The backward SHG signal was collected by the same objective and detected by a HyD detector using a 430-450 nm bandpass. Transmitted light (TL) images of tissue were generated by scanning the sample with a tunable white light laser (WLL) set to 550 nm. SHG and TL images of the same field of view were acquired sequentially.

Supplementary Figure 1

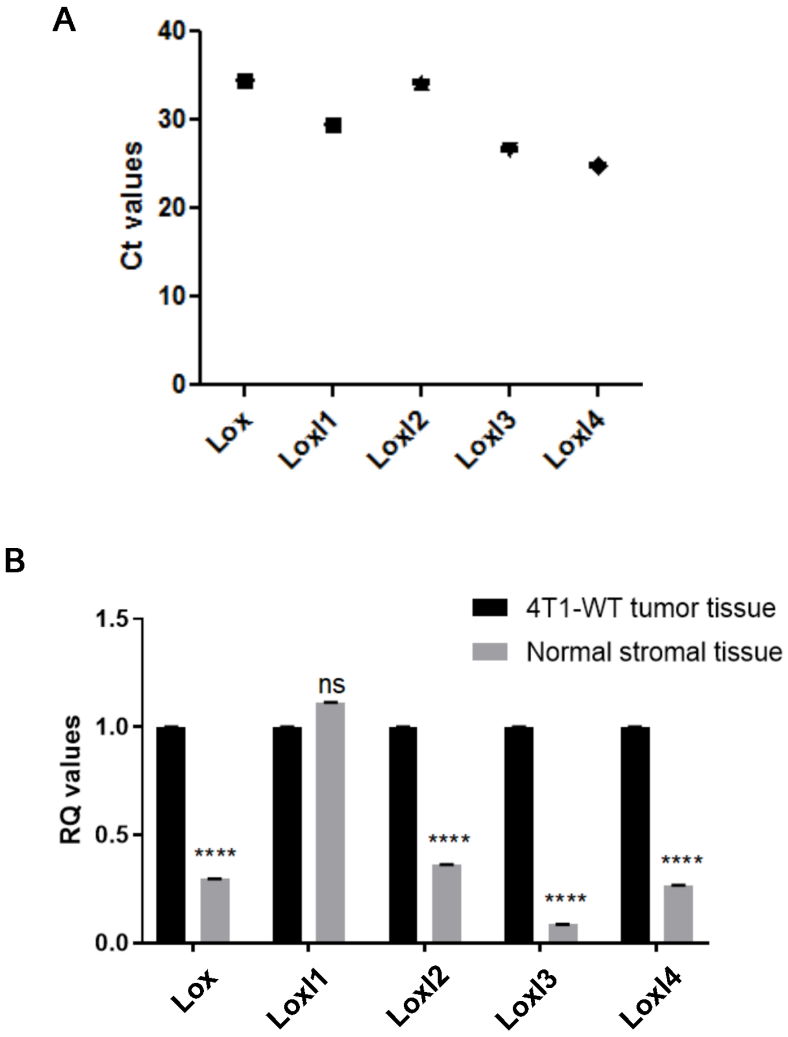

Fig. S1. Expression of LOX family members in 4T1-WT cultured cells and tumors. (A).The mRNA of each LOX family member was detected in triplicate by qRT-PCR in cultured 4T1-WT cells and normalized against GAPDH. (B) Relative expression of each LOX family member in 4T1-WT primary tumors and adjacent stromal tissue normalized against GAPDH (mean ± SEM; ****$p < 0.0001$; n = 4 tumors from different mice; ns = not significant).

Supplementary Figure 2

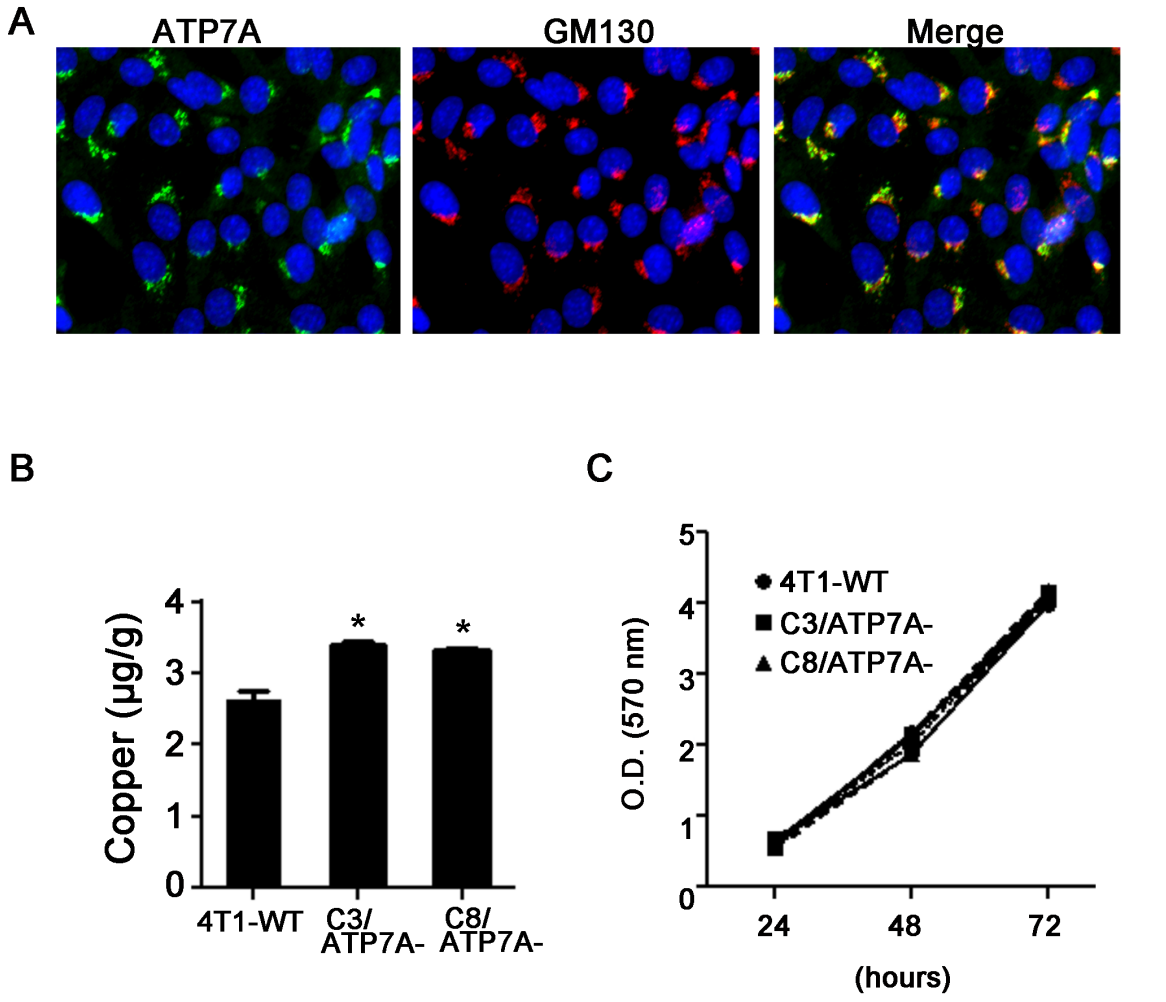

Fig. S2. Characterization of 4T1 cells lacking ATP7A. (A) Detection of ATP7A protein in the Golgi complex of 4T1 cells by immunofluorescence microscopy. ATP7A protein (green) was predominantly detected in the perinuclear region and overlapped with the Golgi marker protein, GM130 (red). Nuclei were labeled with DAPI (blue). (B) Loss of ATP7A results in hyperaccumulation of copper in 4T1 cells. ICP-OES was used to detect cellular copper levels in 4T1-WT, C3/ATP7A- and C8/ATP7A- cells (mean ± SEM; *$p < 0.05$). (C) Loss of ATP7A does not affect cell proliferation in vitro. Cells were cultured in triplicate in basal media for the indicated times. Cell proliferation was measured by the MTT assay (mean ± SEM).

Supplementary Figure 3

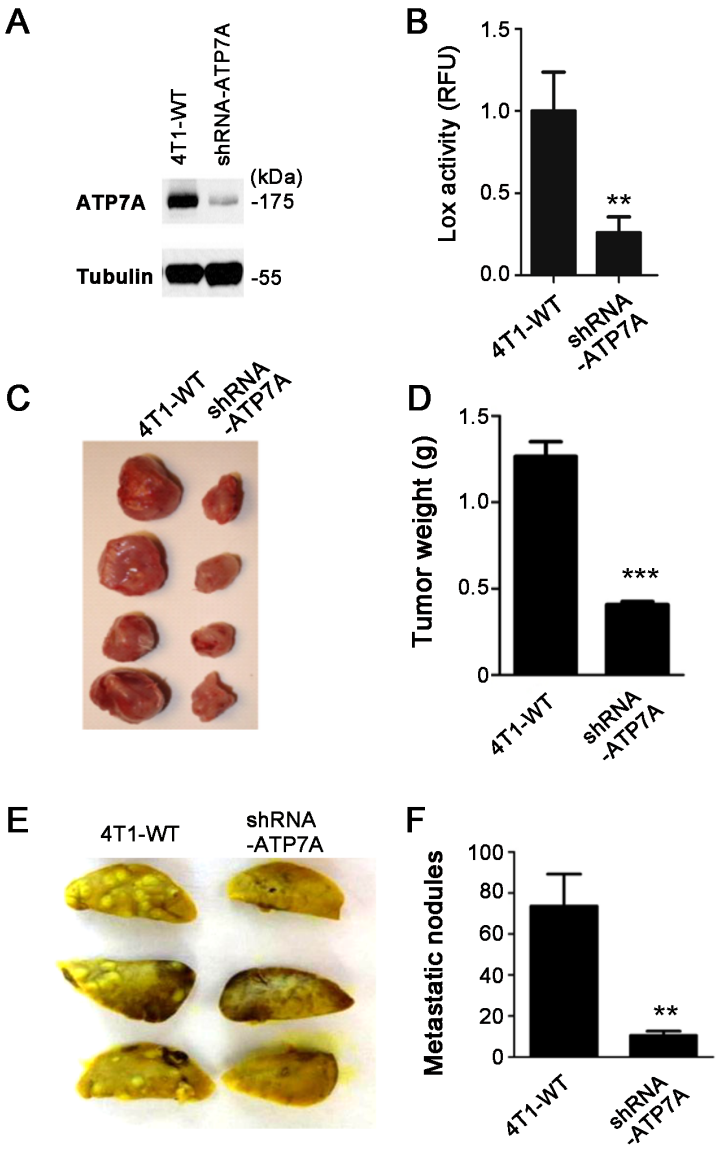

Fig. S3. RNAi-mediated silencing of ATP7A in 4T1 cells suppresses tumor growth and metastasis. (A) Western immunoblot analysis of ATP7A protein in whole cell lysates from 4T1 cells transfected with an shRNA plasmid against GFP (4T1-WT) or against ATP7A (shRNA-ATP7A). Tubulin was detected as a loading control. (B) LOX activity is diminished in the conditioned media from shRNA-ATP7A cells compared to 4T1-WT cells. Activity is expressed as relative fluorescence units (RFU) normalized against 4T1-WT at 24 h (mean ± SEM; **$p < 0.01$). (C and D) Silencing of ATP7A reduces tumor growth in 4T1 cells. The 4T1-WT and shRNA-ATP7A cells were injected subcutaneously into the mammary gland of BALB/c mice (n = 8 per group). Representative images (C) and weights of the primary tumors (D) are shown (mean ± SEM; ***$p < 0.001$). (E) Metastatic lung nodules in mice bearing 4T1-WT and shRNA-ATP7A tumors. Nodules were identified by staining lungs with Bouin's solution. F) Quantification of lung nodules per mouse (mean ± SEM; **$p < 0.01$; n = 8 mice per cell line).

Supplementary Figure 4

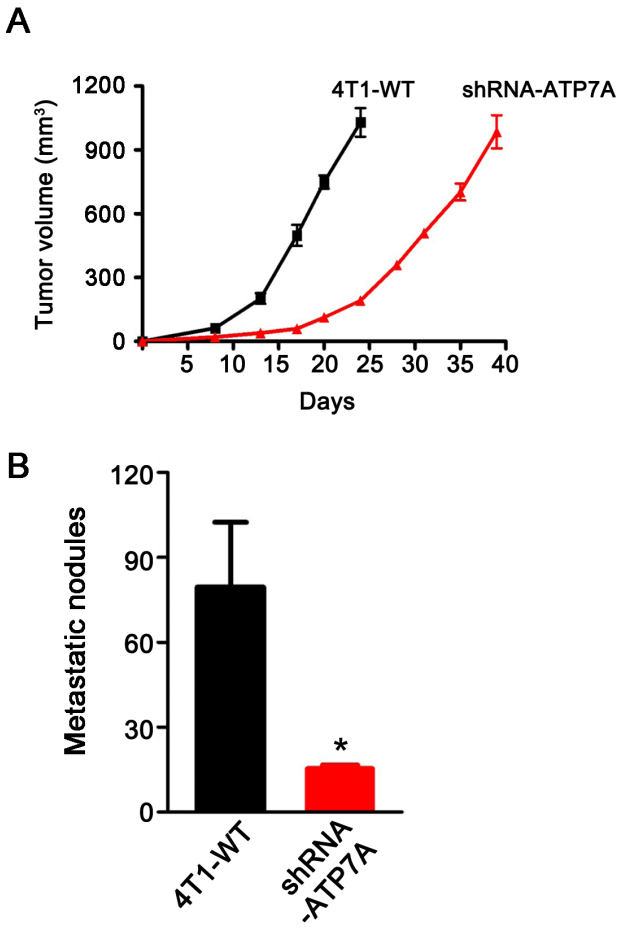

Fig. S4. The reduced metastatic potential of ATP7A-silenced 4T1 cells is independent of primary tumor size. (A) 4T1-WT and shRNA-ATP7A tumors were grown in the mammary glands of BALB/c mice for 24 days or 39 days, respectively, in order to achieve equal primary tumor volumes (mean ± SEM; n = 10 per group). (B) Metastatic lung nodules were enumerated in these mice (mean ± SEM; *$p < 0.05$).

Supplementary Figure 5

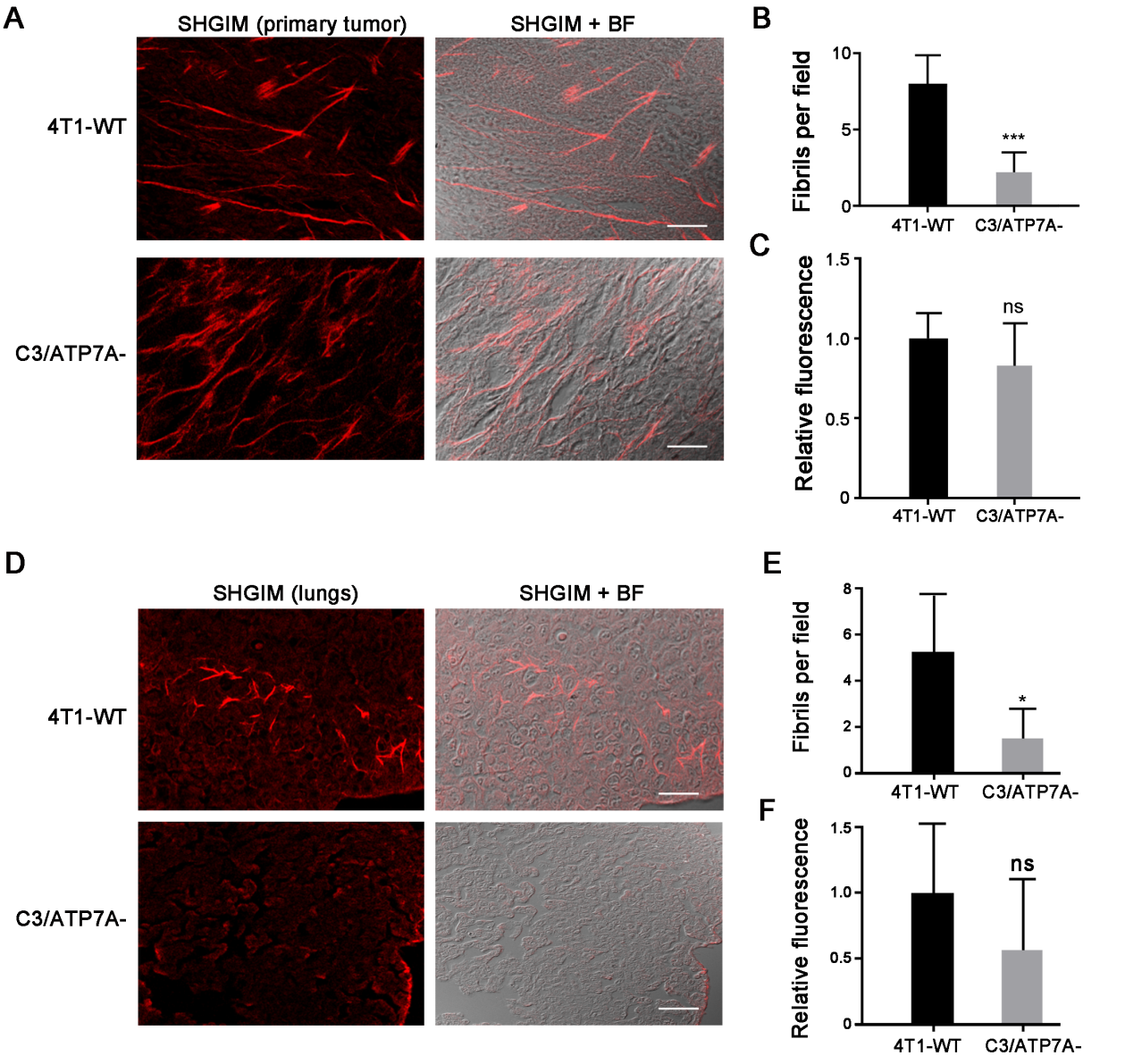

Fig. S5. ATP7A silencing alters collagen fibril assembly *in vivo*. (A) Representative images of collagen signals in primary tumors captured by second harmonic generation imaging microscopy (SHGIM). (B) Quantification of fibrils greater than 30 μm in length per field (mean ± SEM; ***$p < 0.001$; n = 10 fields for 5 tumors per genotype). (C) Fluorescence intensity relative to 4T1-WT cells (mean ± SEM; n = 10 fields for 5 tumors per genotype). (D) Representative SHGIM images derived from the lungs of mice bearing 4T1-WT and C3/ATP7A- tumors. (E) Quantification of fibrils greater than 30 μm in length per field (mean ± SEM; *$p < 0.05$; n = 10 fields for 5 lungs per genotype). Bright field (BF); bars = 20 μm. (F) Fluorescence intensity relative to 4T1-WT cells (mean ± SEM; n = 10 fields for 5 tumors per genotype).

Supplementary Figure 6

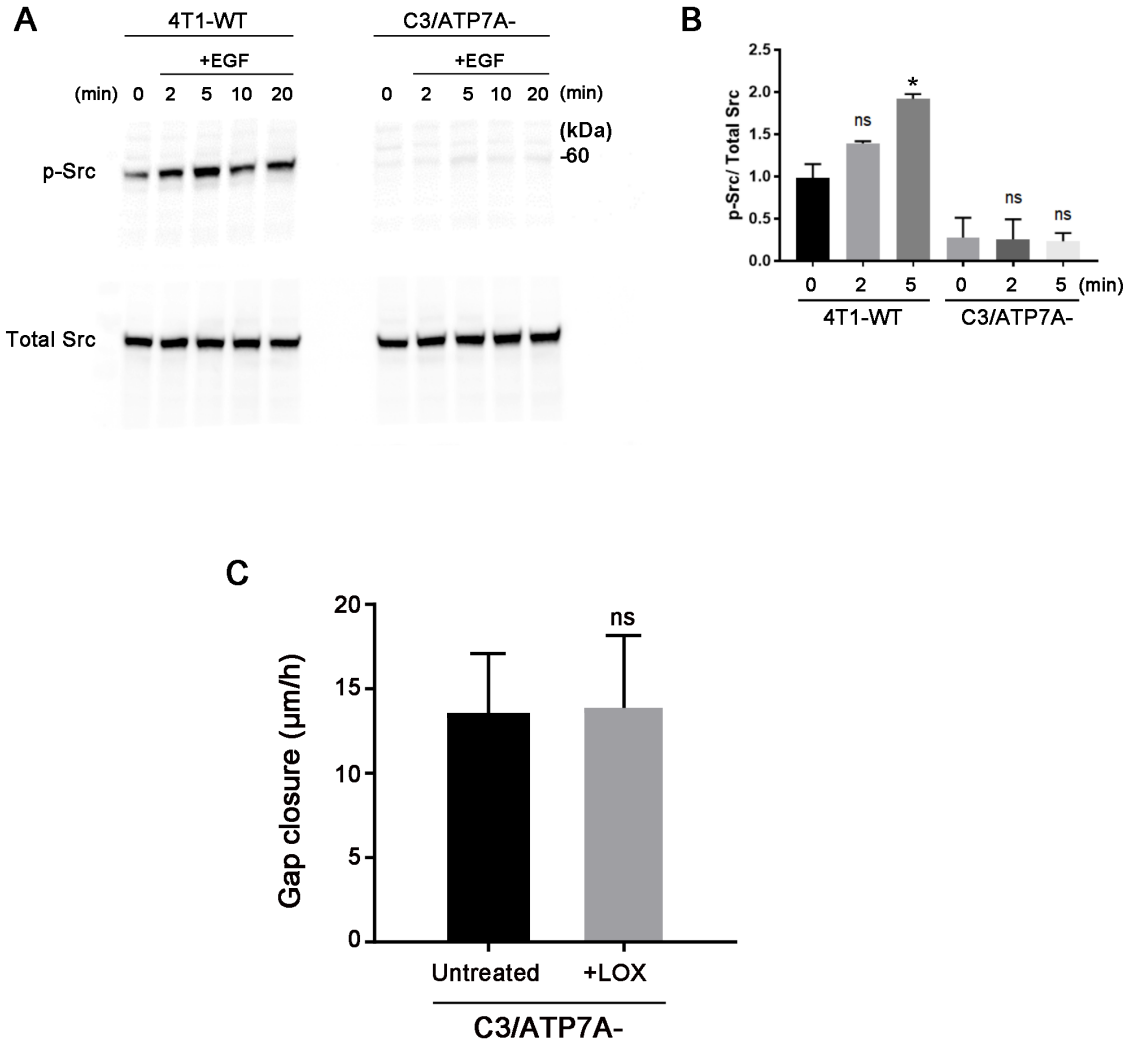

Fig. S6. Characterization of ATP7A-null 4T1 breast carcinoma cells. (A) Immunoblot analysis of Src phosphorylation in 4T1-WT and C3/ATP7A- cells. Cultured 4T1-WT and C3/ATP7A- cells were treated with 10 ng/ml EGF for the indicated times. The abundance of phosphorylated Src (p-Src) and total Src was determined by immunblot analysis. (B) Quantification of the ratio of p-Src to total Src in three independent experiments shown in (A). Values were normalized against untreated 4T1-WT (mean ± SEM; *$p < 0.05$; ns = not significant). (C) Analysis of the effect of exogenous lysyl oxidase (LOX) on cell motility using the scratch assay. Purified human LOX (1 µg/ml) was added to the media of C3/ATP7A- cells after creating a scratch through the monolayer. The rate of gap closure was compared to that of untreated C3/ATP7A- cells (ns = not significant).

Supplementary Figure 7

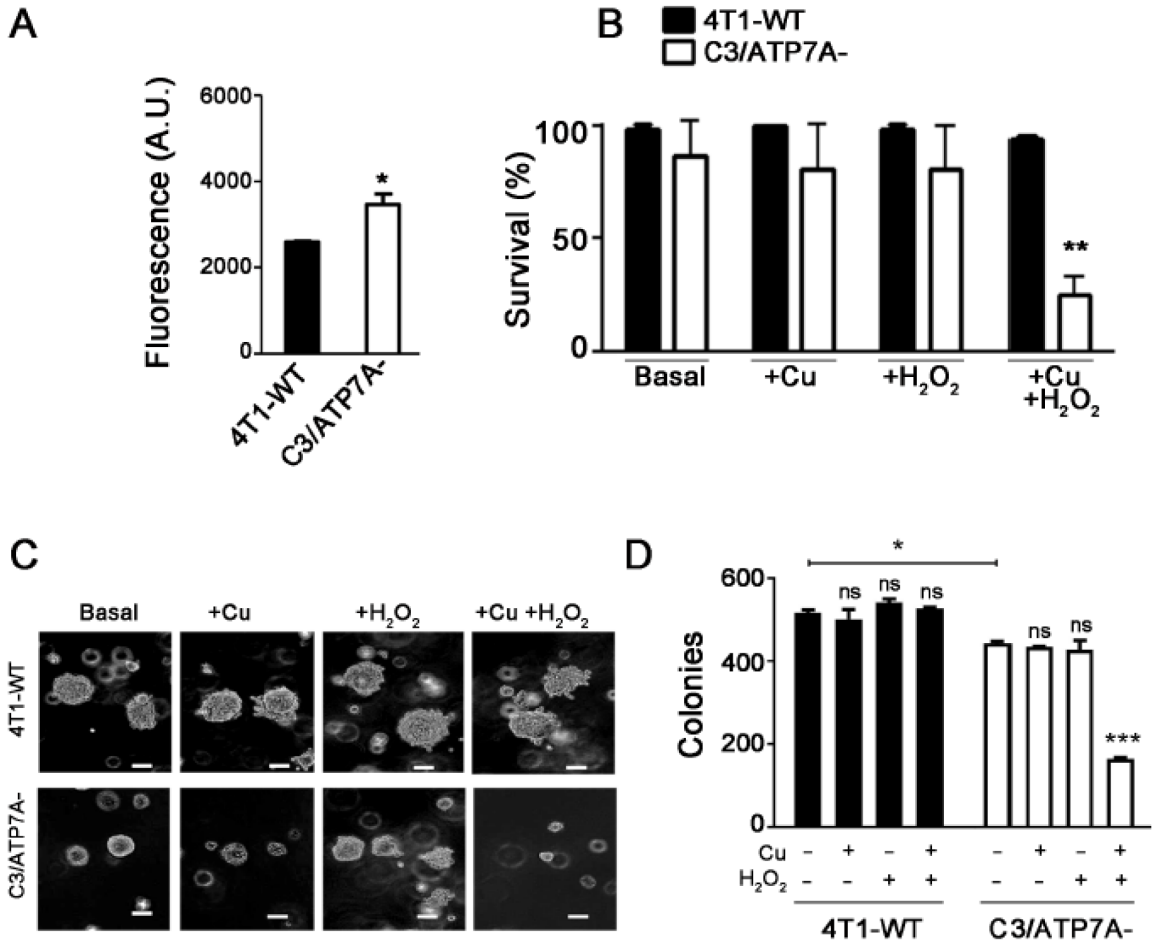

Fig. S7. ATP7A silencing elevates ROS levels and increases sensitivity to subtoxic concentrations of copper and H_2O_2. (A) ROS levels measured in cultured 4T1-WT and C3/ATP7A- cells (mean ± SEM; *p < 0.05; n = 3 experiments in triplicate; RFU, relative fluorescence units). (B) Loss of ATP7A sensitizes cells to subtoxic concentrations of copper and H_2O_2. Cultured 4T1-WT and C3/ATP7A- cells were treated for 48 h with $CuCl_2$ (40 μM) or H_2O_2 (80 μM) alone or in combination. Cell survival was then determined using the Crystal Violet assay (mean ± SEM; **p < 0.01; n = 3 experiments in triplicate). (C) Copper and H_2O_2 synergize to inhibit colony formation of ATP7A-null cells, but not 4T1-WT cells. Representative images of colonies formed in a soft agar assy of 4T1-WT and C3/ATP7A- cells treated for 14 days with $CuCl_2$ (40 μM) or H_2O_2 (80 μM) alone or in combination. Bars = 100 μm). (D) Quantification of colonies in (C) greater than 100 μm in diameter per 10 cm^2 (mean ± SEM; *p < 0.05; ***p < 0.001; n = 5 experiments in triplicate).

Movie S1. *In vitro* scratch assay demonstrating motility of 4T1-WT breast carcinoma cells over a 24 h period.

Movie S2. *In vitro* scratch assay demonstrating reduced motility of C3/ATP7A- breast carcinoma cells over a 24 h period.

Supplementary References

1. Borowicz S*, et al.* (2014) The soft agar colony formation assay. *J Vis Exp* (92):e51998.